Tetrathiafulvalene Vinylogue–Fluorene Co-oligomers: Synthesis, Properties, and Supramoleclar Interactions with Carbon Nanotubes

ARTICLE *in* THE JOURNAL OF ORGANIC CHEMISTRY · JULY 2015

Impact Factor: 4.72 · DOI: 10.1021/acs.joc.5b00792 · Source: PubMed

2 AUTHORS, INCLUDING:

Mohammadreza Khadem

Memorial University of Newfoundland

7 PUBLICATIONS **1** CITATION

SEE PROFILE

JOC The Journal of Organic Chemistry

Article

pubs.acs.org/joc

Tetrathiafulvalene Vinylogue–Fluorene Co-oligomers: Synthesis, Properties, and Supramoleclar Interactions with Carbon Nanotubes

Mohammadreza Khadem and Yuming Zhao*

Department of Chemistry, Memorial University, St. Johns, NL A1B 3X7, Canada

Supporting Information

ABSTRACT: A series of bis(dithiafulvenyl)-end-capped fluorene derivatives was prepared and subjected to a one-pot iodine-promoted oxidative polymerization to yield π-conjugated co-oligomers containing tetrathiafulvalene vinylogue and fluorene repeat units. The resulting π-oligomers were characterized to take either acyclic or cyclic molecular structures, depending on the π-conjugation length of the monomer used for the polymerization. Electronic and electrochemical redox properties were examined by UV–vis spectroscopic and cyclic voltammetric analyses, while the supramolecular interactions of the π-oligomers with single-walled carbon nanotubes were investigated by UV–vis–NIR and Raman spectroscopy.

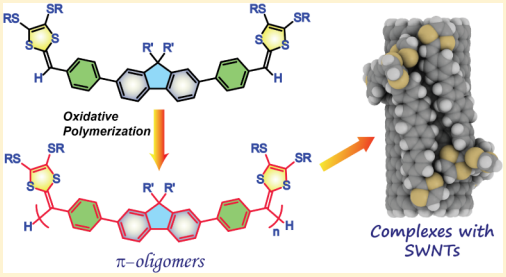

INTRODUCTION

Redox-active π-conjugated oligomers and polymers have offered numerous exciting prospects in the current materials science and nanotechnology,[1] on the basis of which active research has been dedicated to the development of molecular wires,[2] organic photovoltaics,[3] electrochromic devices,[4,5] molecular switches,[6] chemical sensors,[7] and stimuli-responsive materials and soft actuators[8,9] in recent years. A commonly employed strategy to impart desired redox-activity to π-conjugated oligomers and polymers is to have electron donors and/or acceptors either appended to the polymer side chain or placed directly in the repeat unit through π-conjugation.[1] Tetrathiafulvalene vinylogues (TTFVs) are a class of π-extended analogues of the well-known organic electron donor, tetrathiafulvalene (TTF).[10] TTFVs can not only serve as excellent π-electron donors with tunable redox potentials but also show unique redox-triggered conformational switching properties.[11] The interesting molecular properties of TTFVs have sparked surging research interest in developing new TTFV-based functional materials over the past few years, including conjugated polymers,[9,12] macrocycles,[5] switchable ligands,[13] molecular rotors,[14] and chemosensors.[15] TTFV derivatives with aryl groups substituted at the vinylic positions are versatile building blocks for various TTFV-containing π-conjugated systems. The aryl-substituted TTFVs can be made via an oxidative coupling reaction in which a certain dithiafulvene (DTF) precursor is dimerized through a radical mechanism as exemplified by the dimerization of a phenyl-DTF in Scheme 1.[16] The synthetic scope of this methodology encompasses numerous aryl-substituted DTFs,[17,18] wherein the presence of aryl groups facilitates the formation of DTF radical cation in the first step of the mechanism and enables the molecular structure to be further elaborated into diverse π-conjugated motifs.

Scheme 1. General Mechanism for the Oxidative Dimerization of a Phenyl-DTF

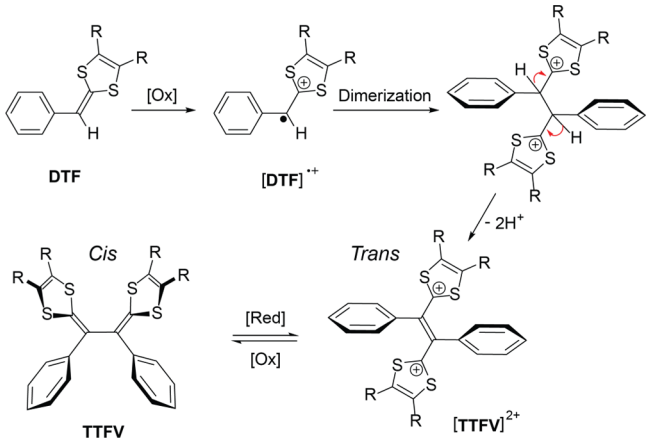

The DTF dimerization reaction provides an efficient C–C bond forming approach through which π-conjugated oligomers and polymers with diverse 1D and 2D structures can be conveniently assembled under either chemical or electrochemical conditions using suitably designed aryl-substituted DTFs as precursors.[9,12,19] Scheme 2 depicts the oxidative polymerization of a generic bis(DTF)-π building block **I**, which leads to the formation of a linear cationic polymer **III**.[20] Subsequent reductive workup yields the neutral polymer product with a TTFV moiety embedded in each of its repeat units. Typically, such a one-pot polymerization reaction as shown in Scheme 2 should give a mixture of polymers with varied chain lengths, whereas precise control over the degree of polymerization is usually not an easy task to accomplish. For

Received: April 21, 2015

DOI: 10.1021/acs.joc.5b00792
J. Org. Chem. XXXX, XXX, XXX–XXX

Scheme 2. General Polymerization Route Using DTF Oxidative Dimerization as the Key Step for Polymer Chain Growth

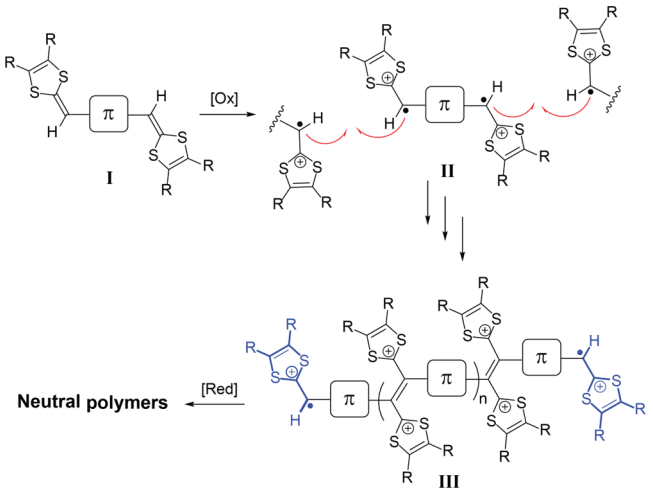

instance, in our previous studies, bis(DTF)-end-capped π-conjugated butadiyne and octatetrayne derivatives were polymerized in solution using iodine as oxidant.[5] The reactions resulted in the formation of a number of relatively short oligomers rather than long-chain polymers. The observed low polymerization degree can be rationalized by noting that when the polymer chain is elongated the terminal DTF groups gradually lose the reactivity toward oxidative dimerization as a result of increased π-delocalization and intermolecular electrostatic repulsion.

The poor efficiency found in DTF polymerization, on the other hand, might suggest a useful synthetic route to prepare relatively short, structurally defined TTFV-based π-oligomers. Hypothetically, if the bis(DTF)-π precursor possesses a moderate reactivity toward DTF oxidative dimerization, it is likely for the terminal DTF radical cations (highlighted by blue color in Scheme 2) to become completely inert toward the oxidation dimerization when the oligomer chain arrives at a certain "critical length". If such a scenario holds true, the polymerization after exhaustive reaction will yield π-oligomers with good monodispersity of chain length. One way to tune down the reactivity of a DTF radical cation is to increase the degree of π-delocalization. Linking the DTF group with π-extended arene units presents a feasible means to attain this goal. Another possible outcome for the one-pot polymerization is the formation of cyclic products, namely macrocycles. TTFV-based macrocycles were rarely reported in the literature. In our recent work, we synthesized a series of trimeric TTFV macrocycles via a one-pot Pd/Cu-catalyzed alkynyl homocoupling of acetylenic TTFV precursors.[5] The DTF oxidative dimerization reaction, however, has not yet been demonstrated as a viable synthetic tool for direct construction of TTFV-containing macrocycles.

This paper addresses the synthetic scope of bis(DTF)-functionalized π-building blocks in terms of making various π-conjugated oligomers and macrocyclic structures. A series of fluorene-centered bis(DTF) derivatives was accordingly designed and synthesized. They were then subjected to a one-pot oxidative polymerization in the solution phase, and the resulting TTFV–fluorene co-oligomers were characterized by electrochemical and UV–vis analyses to understand their redox and electronic properties. Moreover, the supramolecular interactions of these electron-rich conjugated oligomers with single-walled carbon nanotubes (SWNTs) were investigated. π-Conjugated polymers containing TTFV units have been found to give rise to effective and selective dispersion of SWNTs in organic solvents.[9] Herein, the study of SWNT dispersion with TTFV–fluorene co-oligomers will further expand the application scope of TTFV-based π-oligomers in nanoscience and supramolecular chemistry.

RESULTS AND DISCUSSION

Synthesis. The synthetic routes to bis(DTF)-fluorenes **5a–c** are described in Scheme 3. 2,7-Dibromofluorenes **1a–c** were, respectively, reacted with boronate **2** via the Suzuki coupling[21] to give dialdehydes **3a–c** in very good yields. Compounds **3a–c** were then subjected to a phosphite-induced olefination reaction[22] with thione **4** to produce bis(DTF)-fluorene derivatives **5a–c**. With **5a–c** in hand, iodine-promoted (ca.

Scheme 3. Synthesis of Fluorene-Cored Bis(DTF) Derivatives 5a–c and Acyclic TTFV–fluorene Oligomers 6a–c

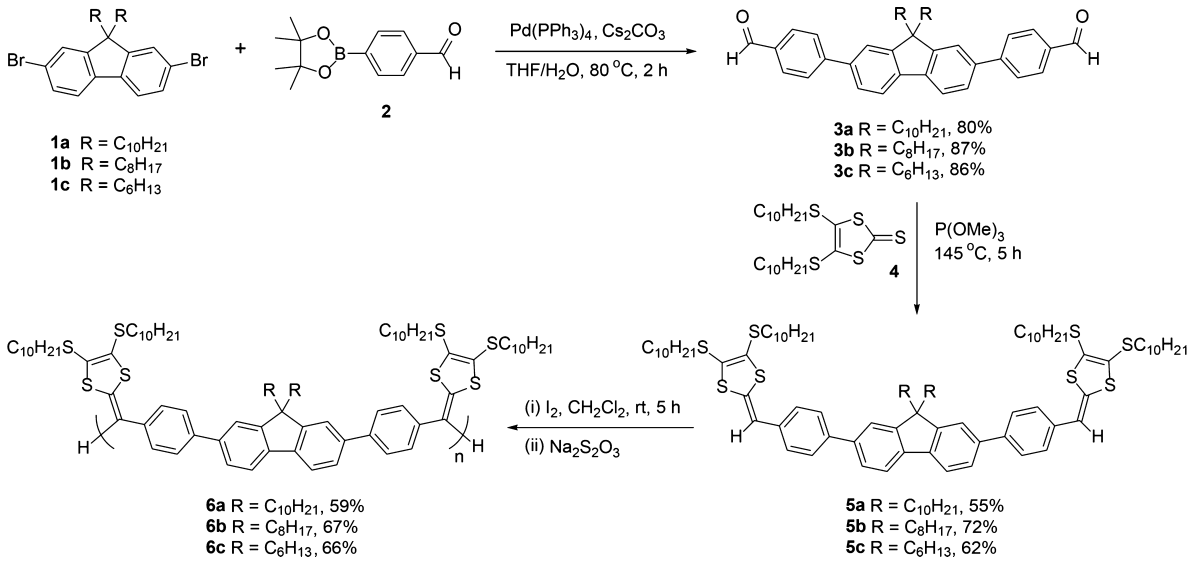

DOI: 10.1021/acs.joc.5b00792
J. Org. Chem. XXXX, XXX, XXX–XXX

Scheme 4. Synthesis of Cyclic TTFV–fluorene Oligomers 10 Using Bis(DTF)-Oligomer 9 as Precursor

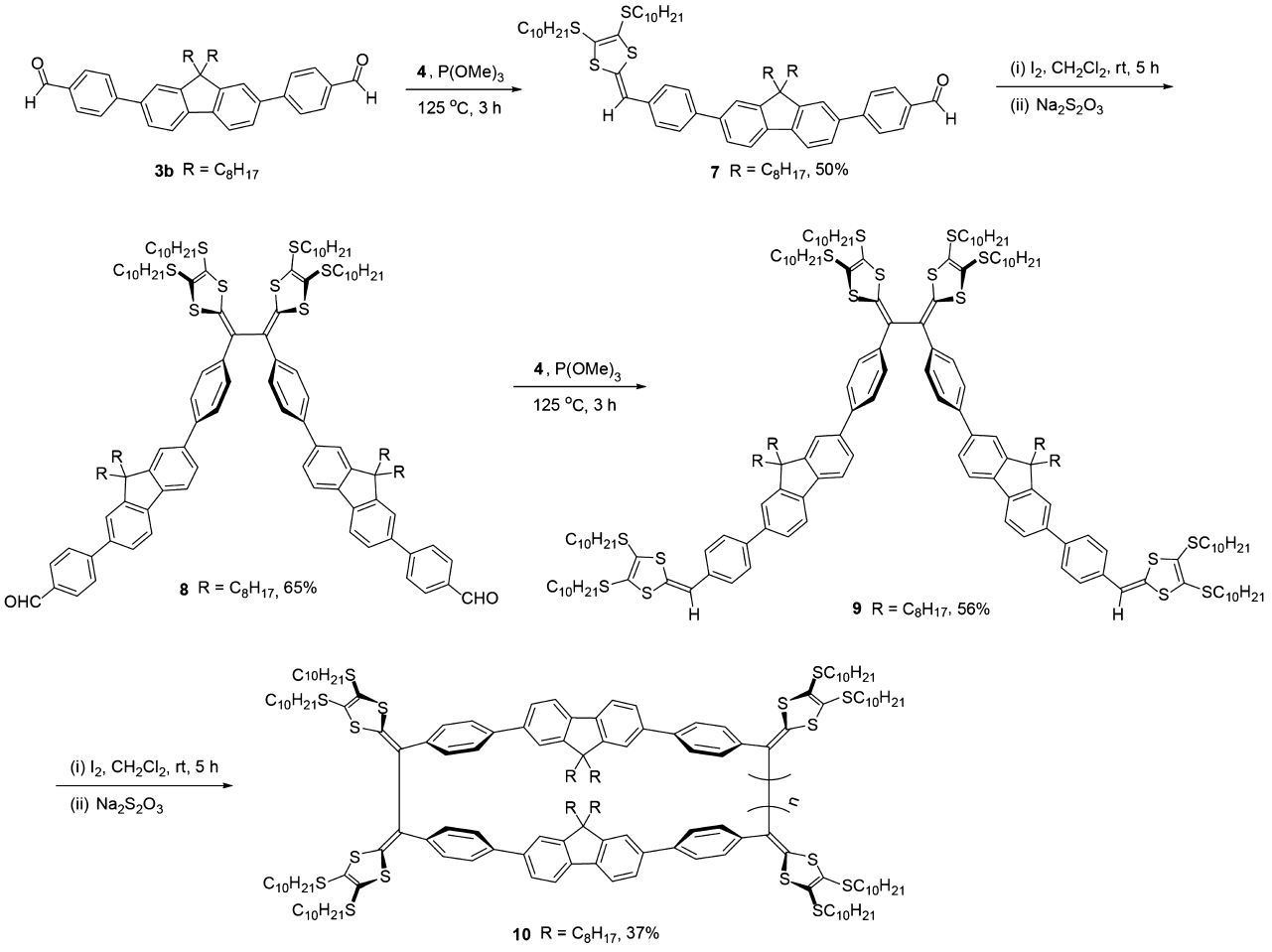

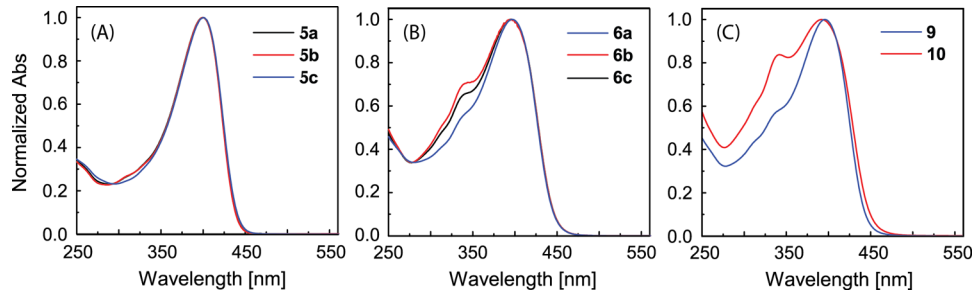

Figure 1. UV–vis spectra of TTFV–fluorene co-oligomers and related π-precursors. All spectra were measured in $CHCl_3$ at room temperature.

2.8 equiv) oxidative polymerization reactions were undertaken in CH_2Cl_2 at room temperature. The reactions in general completed within 5 h, as monitored by thin-layer chromatographic (TLC) analysis. The major products of the polymerization reactions (oligomers **6a–c**) were obtained after a brief reductive aqueous workup with $Na_2S_2O_3$. Careful flash column chromatographic purification then afforded oligomers **6a–c** as brown semisolids in good yields. The molecular structures of these compounds were characterized as the acyclic TTFV–fluorene π-oligomers presented in Scheme 3 on the basis of ^1H NMR, gel-permeation chromatographic (GPC), and cyclic voltammetric (CV) analyses (vide infra).

In addition to the bis(DTF)–fluorenes **5a–c**, the one-pot polymerization was expected to work in a similar way by using bis(DTF)-π precursors with more extended π-skeletons. The resulting oligomers, however, were predicted to have relative higher degrees of polymerization due to the enlarged sizes of the monomers used for polymerization. To further explore in this respect, the synthesis of an extended bis(DTF)-fluorene **9** was pursued as outlined in Scheme 4. Structurally, compound **9** is the dimer of **5b**, but synthetically it is challenging to acquire **9** from direct oxidative dimerization of bis(DTF)-fluorene **5b** due to the presence of two equally reactive DTF groups in **5b**. A multistep synthetic route was hence devised and executed. The synthesis began with an olefination reaction between compound **3b** and with 0.9 equiv of thione **4** in the presence of $P(OMe)_3$ under heating. The major product of this reaction was mono-DTF-substituted compound **7**, which could be easily separated from other byproducts by silica column chromatography. Compound **7** was then subjected to the iodine-induced

DOI: 10.1021/acs.joc.5b00792
J. Org. Chem. XXXX, XXX, XXX–XXX

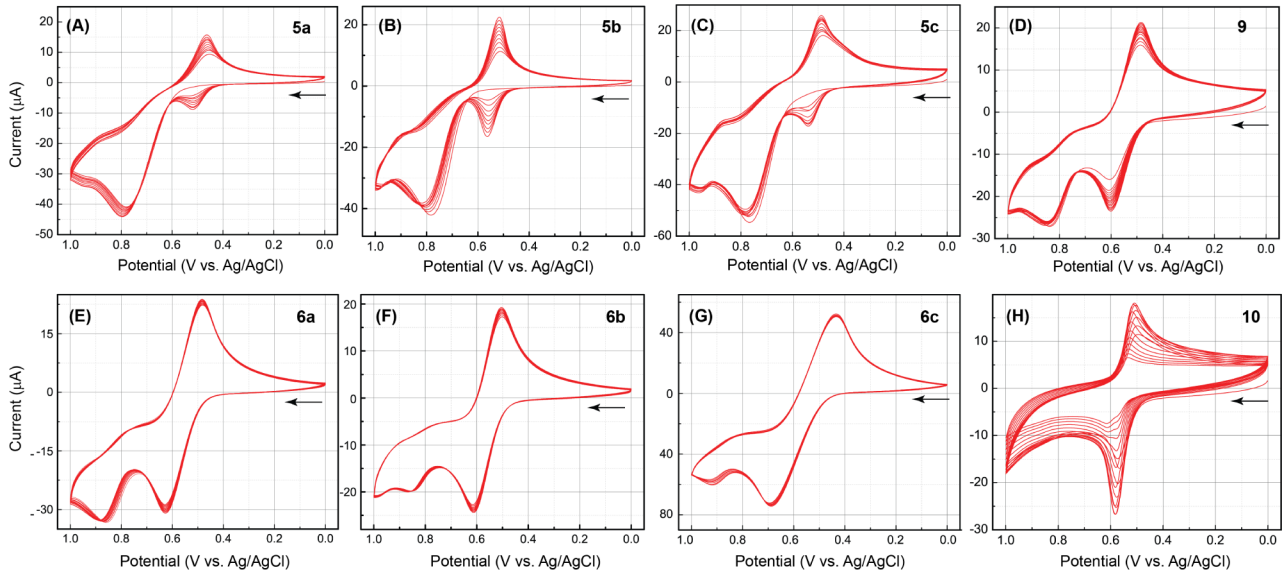

Figure 2. Cyclic voltammograms of compounds **5a−c**, **6a−c**, **9**, and **10** measured in multiple scans. Electrolyte: Bu_4NBF_4 (0.1 M); working electrode: glassy carbon; counter electrode: Pt wire; reference electrode: Ag/AgCl; scan rate: 100 mV s^{-1}.

oxidative dimerization to afford TTFV-centered oligomer **8**. Repetition of the $P(OMe)_3$-promoted olefination on oligomer **8** with thione **4** gave bis(DTF)-oligomer **9** in a satisfactory yield of 56%. Finally, the iodine-induced one-pot polymerization of **9** was performed. To our surprise, there were no significant amounts of acyclic π-oligomers formed out of this reaction; instead, the major products were identified to be in the macrocyclic structure (see **10** in Scheme 4), which was substantiated by ^{1}H NMR, GPC, and CV characterizations (vide infra). Such a synthetic outcome sharply contrasts with the polymerization reactions using relatively shorter bis(DTF)-fluorenes **5a−c** as monomers, while a detailed rationalization for this is made in the later section based on kinetic considerations (see Figure 5).

Electronic and Redox Properties. The electronic absorption properties of the bis(DTF)-fluorene derivatives and related TTFV−fluorene co-oligomers were investigated by UV−vis spectroscopic analysis. Figure 1A shows the UV−vis absorption spectra of bis(DTF)-fluorenes **5a−c**. All of the spectra of the three compounds exhibit a nearly superimposable absorption profile featuring a $\pi \rightarrow \pi^*$ band at 396 nm. Clearly, the side chains attached to the fluorene core barely have any effect on the electronic absorption behavior of the bis(DTF)-fluorene π-framework. The UV−vis spectra of TTFV−fluorene co-oligomers **6a−c** (Figure 1B) show the same absorption band at 396 nm in the low energy region, indicating that the degrees of π-delocalization of the co-oligomers are virtually unchanged in comparison with their bis(DTF)-fluorene precursors. In addition, each of the spectra of **6a−c** exhibits a notable absorption shoulder at 343 nm, which can be assigned to the $\pi \rightarrow \pi^*$ transition of the TTFV units in the oligomer backbones. The UV−vis spectrum of dimer **9** gives a spectral pattern similar to those of co-oligomers **6a−c** (see Figure 1C). In the UV−vis spectrum of macrocyclic oligomer **10** (Figure 1C), the same low energy absorption band at 396 nm can be observed. Unlike the acyclic oligomers **6a−c** and **9**, the shoulder band of macrocycle **10** at 343 nm appears to be significantly stronger in relative intensity, which very likely results from the constraint cyclic π-framework of the macrocycle (see Figure 4). In a comparative study of two dinaphthyl-substituted TTFV isomers we recently reported,[18b] enlargement of the dihedral bond angle between the two vinyl units of TTFV was found to result in significantly increased absorptivity in the spectral range of ca. 330−350 nm. It is therefore deduced that the varied intensity of the shoulder band at 343 nm in the UV−vis spectra of **6a−c** and **10** is tied to the different TTFV conformations in these compounds.

The electrochemical redox properties of the above-mentioned compounds were examined by cyclic voltammetric (CV) experiments, and the detailed cyclic voltammograms are given in Figure 2. The cyclic voltammogram of bis(DTF)-fluorene **5a** (Figure 2A) shows only one anodic peak at +0.78 V in the first cycle of CV scan, which is assigned to the one-electron oxidation of neutral DTF to its radical cation state.[5,16] In the reverse scan, a cathodic peak emerges at +0.46 V, the origin of which is attributed to the reduction of the TTFV dication resulting from the electrochemical dimerization taking place on the working electrode surface.[5,16] As the number of scan cycles increases, another anodic peak is observed to grow steadily at +0.52 V, which is due to the oxidation of the TTFV product accumulated on the working electrode surface. The CV profiles of bis(DTF)-fluorenes **5b** and **5c** (Figure 2B,C) exhibit a similar pattern to that of **5a**, indicating that the three bis(DTF)-fluorene compounds have similar redox activities and electrochemical properties.

The cyclic voltammogram of TTFV−fluorene co-oligomer **6a** gives two anodic peaks at +0.63 and +0.87 V respectively, while in the reverse scan a cathodic peak at +0.44 V is observed (Figure 2E). The first anodic peak and the cathodic peak are due to the reversible redox couple of the TTFV moieties in the co-oligomer, and the second is assigned to the oxidation of the terminal DTF groups of **6a**.[5,16] After being scanned with multiple cycles, these redox peaks do not show any significant changes, indicating that the termianl DTF groups in **6a** are virtually unreactive toward oxidative dimerization. Similar electrochemical redox behavior can be observed in the CV profiles of co-oligomers **9**, **6b**, and **6c** (Figure 2D,F,G); however, the oxidation currents due to the TTFV and DTF moieties show notable differences in relative intensity in the cyclic voltammograms of **6a−c**, and these results can be

DOI: 10.1021/acs.joc.5b00792
J. Org. Chem. XXXX, XXX, XXX−XXX

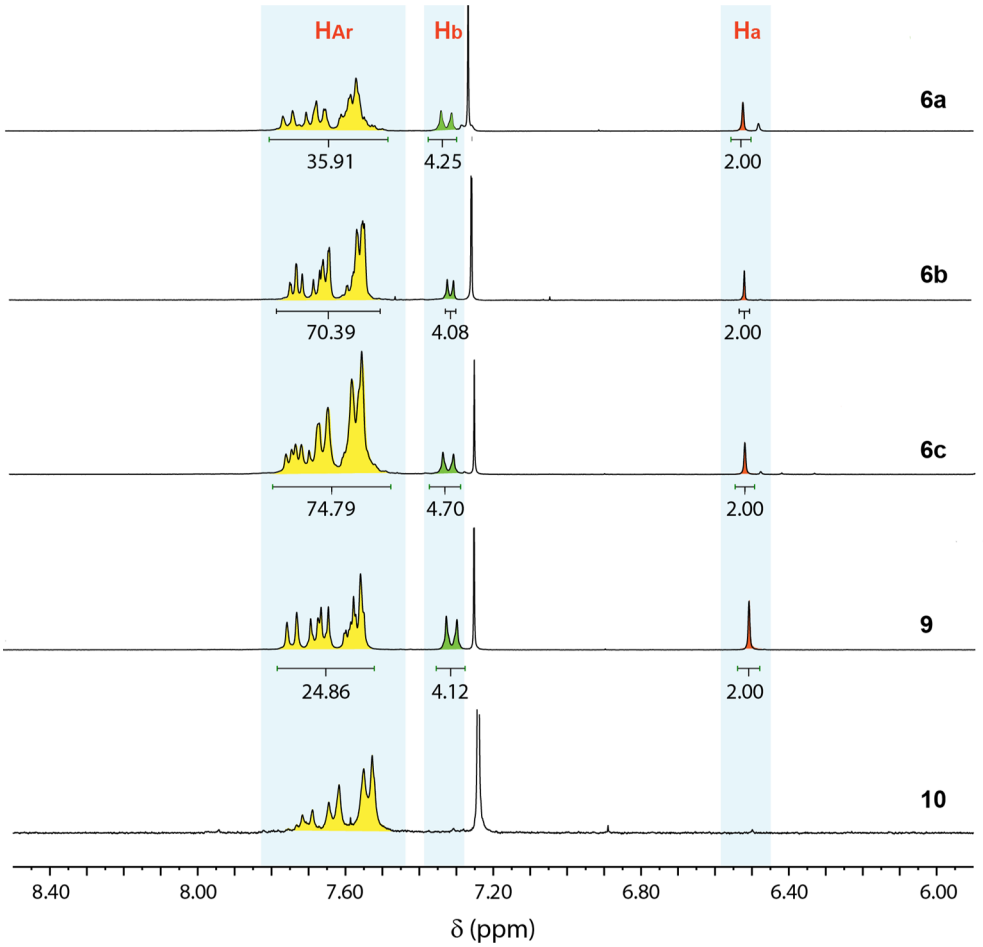

Figure 3. Partial ^{1}H NMR spectra of **6a−c**, **9**, and **10** showing the aromatic and vinylic regions as well as relative integration values therein. The singlet at 7.24 ppm in each spectrum is due to residual $CHCl_3$.

correlated with their different degrees of oligomerization (vide infra). The cyclic voltammogram of macrocycle **10** (Figure 2H) shows only a reversible redox couple at E_{pa} = +0.58 V and E_{pc} = +0.51 V in the first cycle of CV scans, which is characteristic of the TTFV moieties in macrocycle **10**. There is no anodic peak due to DTF oxidation observed in the multicycle CV scans of **10**, which is congruous with the macrocyclic structure. It is also noted that the intensities of the redox wave pair give a significant decreasing trend with increasing number of CV scans, while the redox potentials appear to shift anodically in a slight degree. Such CV behavior alludes to a low degree of electrochemical stability for TTFV−fluorene macrocycle **10**.

Structural Elucidation of TTFV−Fluorene Co-oligomers. As manifested by the CV analysis, the structures of TTFV−fluorene co-oligomers **6a−c** take an acyclic structure with two DTF groups end-capped at the termini of each oligomer chain. The structure of co-oligomer **10**, on the other hand, is deduced to be in a macrocyclic motif based on the absence of DTF oxidation peaks in its cyclic voltammogram. For these co-oligomers, determination of the degrees of oligomerization (n, as indicated in the structures of co-oligomers shown in Schemes 3 and 4) is of great importance to better understanding their structural properties as well as gaining mechanistic insight into the oxidative polymerization reactions.

^{1}H NMR analysis has proven to be an indispensable tool for determination of the n values in acyclic co-oligomers **6a−c**, given that the unique chemical shift of the vinylic protons (H_a) on the terminal DTF groups is distinctively separated from the other aromatic protons on the oligomer backbone. Figure 3 shows the partial ^{1}H NMR spectra of **6a−c**, **9**, and **10**, highlighting the aromatic and vinylic regions. In each of the spectra, the vinylic protons of the terminal DTF groups (H_a) give a singlet at 6.51 ppm. In addition, a pseudo doublet (labeled as H_b) can be clearly seen at 7.31 ppm. The origin of H_b can be assigned to the *ortho*-protons on the phenyl ring adjacent to the terminal DTF group. Other aromatic protons located on the fluorene and phenyl rings (H_{Ar}) collectively contribute to the signals in the range of 7.49−7.76 ppm, which are too significantly overlapped to attain detailed assignments. The integral ratio of H_a versus the sum of H_b and H_{Ar} thus allows the average degree of oligomerization (n) for each co-oligomer to be calculated (see Table 1). The NMR results show

Table 1. Summary of GPC Data for TTFV−fluorene Co-Oligomers and Their Calculated Degrees of Oligomerization (n)

entry	M_n	M_w	PDI	M_n/M_0	n(calcd, NMR)	n(calcd, CV)
6a	4392	6965	1.39	3.13	2.87	3.29
6b	7961	12303	1.54	5.45	5.32	5.45
6c	8200	11119	1.35	5.41	5.63	8.31
9					2.07	1.93
10	3126	7297	2.33	1.07		

DOI: 10.1021/acs.joc.5b00792
J. Org. Chem. XXXX, XXX, XXX−XXX

that co-oligomers **6b** and **6c** have similar oligomerization degrees (i.e., at the stage of pentamer to hexamer). Comparatively, co-oligomer **6a** has a relatively lower degree of oligomerization (n = 2.87), suggesting that the dominant component of **6a** is trimer. The relative lower oligomerization degree of **6a** can be ascribed to the long side chains on the fluorene units, the increased steric hindrance of which may retard the oxidative oligmerization.

The ^{1}H NMR analysis on the average degree of oligomerization (n) was then compared with gel permeation chromatographic (GPC) data. As listed in Table 1, TTFV−fluorene co-oligomers **6a−c** all exhibit relatively narrow polydispersity (PDI = 1.3−1.5). The degree of oligomerization (n) can be worked out using the formula $n = M_n/M_0$, where in M_n is the number-average molecular weight determined by GPC and M_0 is the molecular weight of the monomer used for the polymerization. The degrees of oligomerization calculated for **6a−c** based on GPC data show a good agreement with those derived from NMR analysis, testifying to the reliability of both methods in elucidating the structures of bis(DTF)-end-capped TTFV−fluorene co-oligomers. The GPC data for macrocycle **10** gave an M_n value very close the molecular weight of dimer **9**, indicating that the dominant reaction pathway in the macrocyclization of **9** was a ring closure resulting from intramolecular coupling of the two terminal DTF groups rather than intermolecular expansion. Nevertheless, the relatively wide polydispersity (PDI = 2.33) measured for **10** suggests that larger macrocycles were also formed via intermolecular cycloaddition pathways to a certain extent. The molecular structure of the macrocycle resulting from the intramolecular cyclization of **9** was simulated by the molecular mechanics (MM) approach using the MMFF force field implemented in Spartan'10 (Wave function, Inc.). As shown in Figure 4, the optimized geometry of the macrocycle shows that the dihedral angle between the two vinyl groups in each of the TTFV moieties is about 76−80°, which is larger than those observed for typical phenyl-substituted TTFV compounds[18] as a result of the macrocyclic strain energy. The two fluorene units are somehow parallelly oriented, but they are not close enough to induce significant van der Waals contact or π-stacking. Moreover, the central cavity of the macrocycle appears to be very small and therefore not suited to encapsulate meaningful molecular guests.

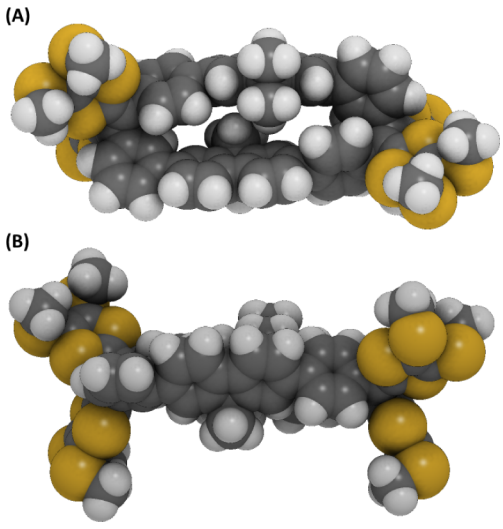

Figure 4. Space-filling model of macrocycle **10** (n = 1) optimized using the MMFF force field: (A) side view, (B) top view. Long alkyl chains were replaced by CH_3 to save computational costs.

Apart from NMR and GPC analyses, the CV data could also serve as a meaningful way to assess the average degree of oligomerization (n) for **6a−c**. As can be seen from Figure 2, the anodic peaks due to the oxidation of DTF and TTFV moieties are well separated from one another in the voltammogram of each oligomer. In principle, a DTF unit releases one electron and a TTFV unit loses two electrons during the oxidation processes. Assuming that the current intensity of each anodic peak is proportional to the number of electrons transferred,[23] the ratio of the current intensities for DTF and TTFV thus offers a quantitative measure for the degree of oligomerization (n). To evaluate the usefulness of this method, the current intensities (i_{pa}) of the DTF and TTFV anodic peaks for TTFV−fluorene dimer **9** were first examined. The calculated n value (1.93) according to the CV data is satisfactorily close to the ideal value (n = 2) for dimer **9**, corroborating the reliability of the electrochemical method (see Table 1). Indeed, the degrees of oligomerization (n) calculated on the basis of the anodic peak currents are consistent with those determined by the GPC and NMR analyses in the cases of co-oligomers **6a** and **6b**. For co-oligomer **6c**, however, the electrochemical analysis yields a slightly larger n value than the other two methods, and the exact reason for such a discrepancy awaits more detailed investigation to clarify. It is worth mentioning that strenuous efforts were made in our work to characterize the TTFV−fluorene co-oligomers by MALDI-TOF MS analysis. Unfortunately, only dimer **9** was reasonably characterized by MS, whereas the other co-oligomers only gave the mass peaks due to smaller fragment ions in their mass spectra. It is therefore reasoned that these oligomers are unstable to the laser shots under the MALDI conditions, resulting in rapid decomposition and fragmentation which in turn obscured the MALDI-TOF MS analysis.

Mechanisms of Polymerization. The various characterization data have congruously indicated that the one-pot oxidative polymerization of bis(DTF)-fluorenes **5a−c** led to the formation of acyclic TTFV−fluorene co-oligomers with relatively narrow polydispersity. In contrast, treatment of compound **9**, which is the dimer in the series of co-oligomer **6b**, under the same oxidative conditions yielded only cyclic products. The different synthetic outcomes suggest that the DTF oxidative polymerization does not follow a conventional polymerization mechanism in which the monomers and/or intermediary oligomers react with each other nonselectively. The fact that dimer **9** predominantly underwent an intramolecular cyclization reaction suggests that the intermolecular DTF coupling between dimers and/or higher oligomers is a sluggish and disfavored pathway in the polymerization mechanism. It is therefore reasonable to propose that the mechanism for the polymerization of **5a−c** predominantly follows the chain-length growth pathway illustrated in Figure 5, in which the monomer is added to each of the termini of the intermediary oligomers in a stepwise fashion. When the oligomer is grown to a "critical chain length" where the terminal DTFs become completely inert to the oxidative dimerization reaction, the polymerization reaction is terminated. As such, the final products of the polymerization should converge toward a peculiar chain length with much better monodispersity than the outcome of a conventional polymerization pathway. Experimentally, the narrow polydispersity of

DOI: 10.1021/acs.joc.5b00792
J. Org. Chem. XXXX, XXX, XXX−XXX

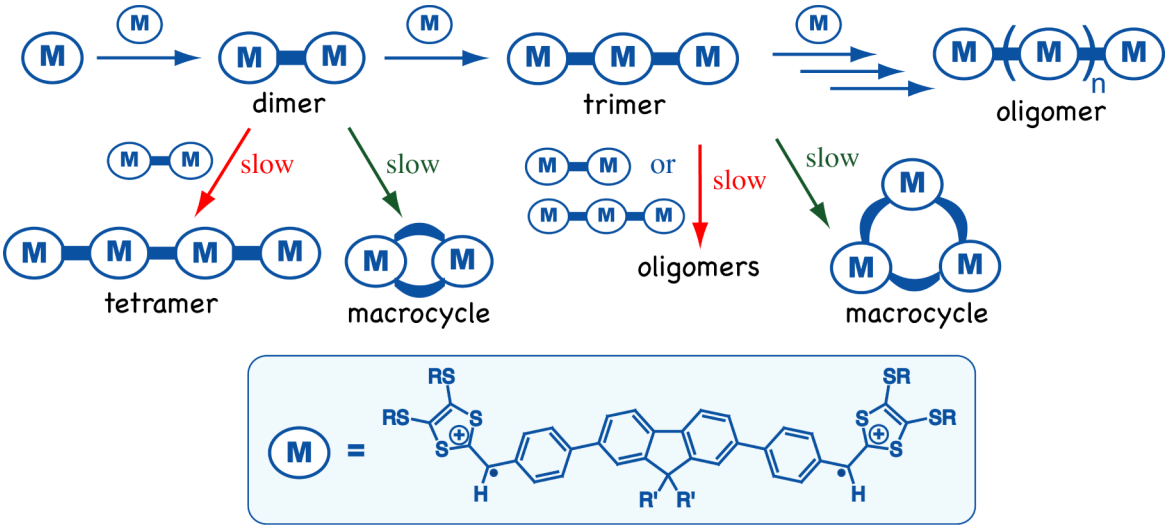

Figure 5. Illustration of different reaction pathways involved in the one-pot oxidative polymerization of bis(DTF)-fluorenes.

co-oligomers **6a–c** determined by GPC analysis attests to the proposed selective chain length growth mechanism. Another valid argument supporting the proposed mechanism is that in the oxidative polymerization of **5b** the first intermediate formed was actually dimer **9** in its oxidized state. If the conventional polymerization mechanism took place in a significant degree, the polymerization of **5b** would also produce macrocyclic oligomer **10** as one of the major products, but this scenario was not observed experimentally.

Supramolecular Interactions of TTFV–Fluorene Co-oligomers with Single-Walled Carbon Nanotubes. The conformational properties of TTFV–fluorene co-oligomers **6a–c** were investigated by molecular mechanics (MM) simulations, where a model co-oligomer featuring the same π-framework as those of **6a–c** but without alkyl side chains was examined. The chain length of the model oligomer was set at the pentamer stage (n = 5) to be consistent with the average oligomerization degrees of co-oligomers **6b** and **6c**. As can be seen from Figure 6A,B, the optimized geometry of the model oligomer adopts a "squarelike" folding structure with a central cavity of ca. 1–2 nm in diameter. Our previous studies have demonstrated that TTFV-containing π-conjugated polymers and bis(DTF) end-capped π-oligomers were able to wrap around or stick to the surface of single-walled carbon nanotubes (SWNTs), resulting in effective and selective dispersion of SWNTs in various organic solvents.[9] Along this line, we further envisioned that the unique folding features of the TTFV–fluorene co-oligomers together with their π-rich conjugated backbones should engender favorable supramolecular interactions with SWNTs. MM simulations of the interactions between the model oligomer and a segmental (10,0) SWNT have revealed a wrapping mode (Figure 6C,D) dictated by intimate π-stacking between the oligomer π-framework and the SWNT surface.

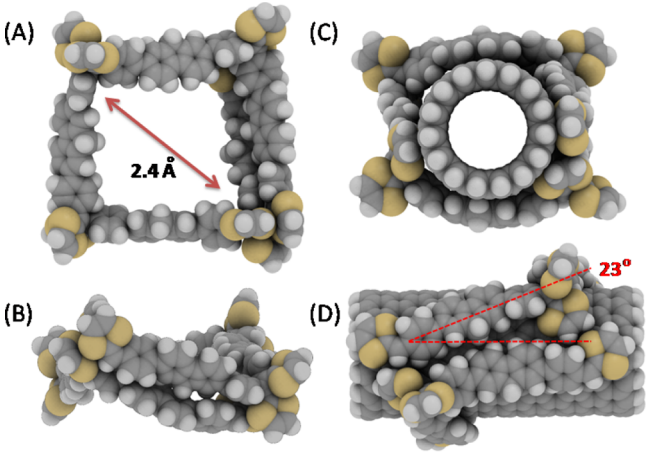

Figure 6. Optimized geometries of a TTFV–fluorene pentamer (A: front view; B: side view) and the oligomer wrapping around a (10,0) nanotube (C: front view; D: side view).

To validate the prediction by the molecular modeling studies, two commercially available SWNT samples (namely, HiPCO and CoMoCAT) were acquired and subjected to dispersion experiments in organic solvents using co-oligomers **6a–c** as dispersing agents. In this work, SWNT dispersion was conducted by the ultrasonication/filtration procedures we reported previously.[9] It was found that all the co-oligomers could effectively disperse HiPCO nanotubes into two common organic solvents, $CHCl_3$ and THF, to form stable suspensions. The effectiveness of dispersion in $CHCl_3$ appeared to be better than in THF. For the CoMoCAT nanotubes, however, there was no significant dispersion observed in common organic solvents.

The HiPCO SWNT suspensions dispersed with co-oligomers **6a–c** in $CHCl_3$ were characterized by UV–vis–NIR analysis, and the results are shown in Figure 7A. The variously distinct absorption bands in the vis–NIR region are characteristic of the interband transitions of debundled SWNTs in the solution.[24] The SWNTs dispersed by the three TTFV–fluorene co-oligomers give nearly superposable spectral patterns in Figure 7A, suggesting that the three π-oligomers have similar selectivity for the types of SWNTs dispersed in $CHCl_3$. In THF, the vis–NIR absorption spectra of the SWNTs dispersed by **6a** and **6b** (see Figure 7B) bear similar features to one another as well as to those determined in $CHCl_3$. For the SWNTs dispersed with oligomer **6c** in THF, however, the vis–NIR spectrum is notably different in comparison with the others. The relatively lower solubility of **6c** than the other two co-oligomers in THF, due to the short

DOI: 10.1021/acs.joc.5b00792
J. Org. Chem. XXXX, XXX, XXX–XXX

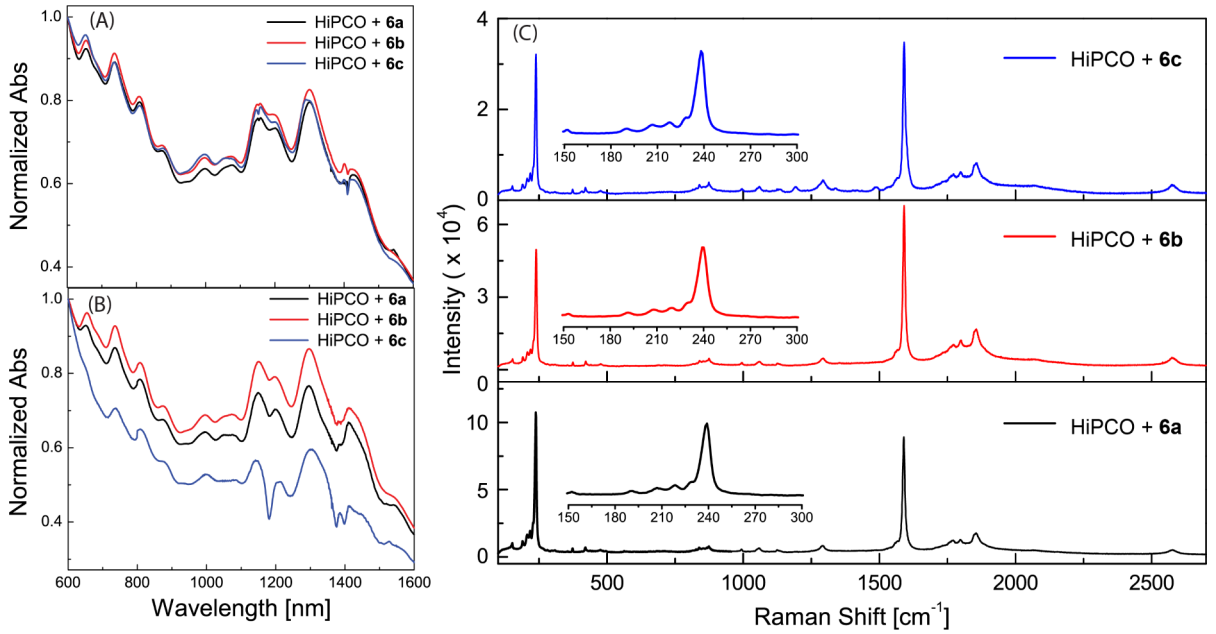

Figure 7. (A) UV−vis−NIR spectra of HiPCO SWNTs dispersed with co-oligomers **6a−c** in $CHCl_3$. (B) UV−vis−NIR spectra of HiPCO SWNTs dispersed with co-oligomers **6a−c** in THF. (C) Raman spectra of SWNTs dispersed with co-oligomers **6a−c**. Insets: Expanded spectra showing the radial breathing mode (RBM) region.

alkyl chains attached to the fluorene moieties, could be a reason for the different spectral features in the vis−NIR region.

To shed more light on the selectivity issue, Raman spectroscopic analysis was conducted. Figure 7C shows the Raman spectra of SWNTs dispersed with **6a−c**. Overall, the three Raman spectra bear close resemblance to one another, in which the dominant features are the tangential G band of SWNTs at 1590 cm^{-1} and a sharp band at 239 cm^{-1} in the radial breathing mode (RBM) region. The two characteristic Raman bands testify to the efficient dispersion of SWNTs by the three co-oligomers.

Figure 8 compares the spectra of oligomer **6b**, raw HiPCO SWNTs, and SWNTs dispersed with **6b**. The Raman spectrum of raw HiPCO SWNTs clearly shows a significant G^- band together with the G^+ band in the tangential mode region. In addition, the D band is discernible at 1329 cm^{-1}. In sharp contrast, the SWNTs dispersed with TTFV−fluorene co-

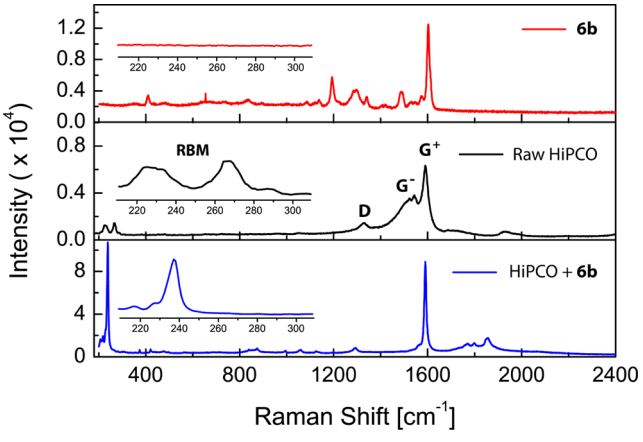

Figure 8. Comparison of the Raman spectra of co-oligomer **6**, raw HiPCO SWNTs, SWNTs dispersed with **6**. Insets: Expanded spectra showing the radial breathing mode (RBM) region.

oligomers do not give any significant G^- band. Moreover, the RBM bands of dispersed SWNTs appear to be much narrower than those of the raw HiPCO SWNTs. The Raman data corroborate that the dispersed SWNTs possess a better quality than raw SWNTs in terms of structural homogeneity; in particular, the diameters of the dispersed SWNTs are found to be narrowly distributed, given that RBM frequency (ω) is inversely proportional to the diameter of SWNT (d).[25] Using the equation $\omega_{RBM} = 248/d$, developed by Dresselhaus et al.,[26] the average diameter (d) of the SWNTs selectively dispersed by **6a−c** in $CHCl_3$ is estimated to be ca. 1.04 nm. Such a good diameter selectivity is believed to arise from the unique wrapping mode of the oligomers with SWNTs as disclosed by the molecular modeling studies. The development of stimuli-responsive oligomers and polymers as SWNT dispersants has become a topic of research recently, and one advantage of this approach that particularly appeals to the application in SWNT-based devices is the ease and effectiveness in regenerating "additive-free" SWNTs after solution-phase processing.[9,27] Along this vein, we expect that the redox-active TTFV−fluorene co-oligomers **6a−c** will find further application in SWNT-based nanodevices and materials.

Conclusions. Oxidative dimerization of aryl-substituted DTFs offers a direct C−C bond-forming approach through which various extended π-conjugated systems can be generated. In this work, bis(DTF)-end-capped fluorenes **5a−c** were used as monomers for the iodine-induced oxidative DTF polymerization, yielding acyclic TTFV−fluorene co-oligomers with narrow polydispersity. The same oxidative reaction conditions applied to the bis(DTF) dimer **9**, however, led to a completely different synthetic outcome, wherein only cyclic oligomer products were formed as a result of the favored intramolecular DTF coupling. Our synthetic work has confirmed that the reactivity of a DTF group toward the oxidative dimerization is highly dependent on the degree of π-conjugation of the aryl group attached to it. Another intriguing discovery is that the mechanism for the oxidative polymerization of bis(DTF)-

DOI: 10.1021/acs.joc.5b00792
J. Org. Chem. XXXX, XXX, XXX−XXX

fluorenes **6a**–**c** follows a selective chain length growth pathway, in which the oligomer intermediates favor to react with the bis(DTF)-fluorene mononers. This unique reactivity has enabled relatively monodisperse π-oligomers to be generated as the major products through the one-pot polymerization approach. Finally, the TTFV–fluorene co-oligomers were demonstrated to give rise to strong supramolecular interactions with SWNTs, which in turn allowed for effective and selective dispersion of SWNTs in the organic solutions of TTFV–fluorene co-oligomers. In summary, the findings disclosed in this work have contributed useful knowledge to the development of new redox-active functional materials based on π-conjugated oligomers and macrocycles.

EXPERIMENTAL SECTION

General Information. Commercially available chemicals were used directly without purification. All reactions were conducted in standard, dry glassware and under an inert atmosphere of nitrogen or argon unless otherwise noted. ^{1}H and ^{13}C NMR spectra were recorded on a 500 MHz or a 300 MHz multinuclear spectrometer. Chemical shifts (δ) are reported in ppm downfield relative to the signals of the internal reference $SiMe_4$ or residual solvent signals from $CHCl_3$ δ = 7.24 ppm and δ = 77.2 ppm, CH_2Cl_2 δ = 5.32 ppm and δ = 54.0 ppm, respectively. Coupling constants (J) are reported in hertz. MALDI-TOF MS analysis was performed in the positive mode using dithranol as the matrix. High-resolution EI-TOF MS analysis was performed in the positive mode. Raman spectroscopic analysis was done on a Raman microscope equipped with a laser source at the wavelength of 830 nm. Gel permeation chromatographic (GPC) analysis was performed using THF as the eluent at a flow rate of 1.0 mL/min and monitored by a photodiode array detector and a refractive-index detector. Polystyrene standards were used for calibration.

4,4′-(9,9-Didecyl-9*H*-fluorene-2,7-diyl)dibenzaldehyde (3a). 2,7-Dibromo-9,9-didecyl-9*H*-fluorene (**1a**) (1.70 g, 2.81 mmol), benzaldehyde **2** (1.60 g, 6.89 mmol), Cs_2CO_3 (14.6 g, 44.8 mmol), and $Pd(PPh_3)_4$ (0.33 g, 0.29 mmol) were added to a 100 mL round-bottom flask. THF (35 mL) and deionized water (15 mL) were added to the flask under an atmosphere of argon. The mixture was refluxed for 2 h under argon. After that, the mixture was cooled to room temperature and then poured into brine. The resulting mixture was extracted twice with CH_2Cl_2. The combined organic layers were dried over $MgSO_4$, and the solvent was evaporated off under vacuum. The residue was crude product **3a**, which was further purified through silica column chromatography (Et_2O/EtOAc 1:4) to give pure **3a** (1.50 g, 2.30 mmol, 80%) as a pale yellow oil: IR (neat) 2921, 2850, 2728, 1697, 1600, 1249, 1210, 812 cm^{-1}; ^{1}H NMR (300 MHz, $CDCl_3$) δ 10.09 (s, 2H), 8.00 (d, J = 8.4 Hz, 4H), 7.86–7.83 (m, 6H), 7.69–7.61(m, 4H), 2.10–2.04 (m, 4H), 1.31–1.11 (m, 32H), 0.82 (t, J = 6.9 Hz, 6H); ^{13}C NMR (75 MHz, $CDCl_3$) δ 191.9, 152.0, 147.5, 140.9, 138.8, 135.1, 130.3, 127.7, 126.5, 121.7, 120.54, 55.5, 40.3, 31.8, 29.9, 29.6, 29.5, 29.3, 29.2, 22.6, 14.1; HRMS [M]$^+$ calcd for $C_{47}H_{58}O_2$ 654.4437, found 654.4418.

4,4′-(9,9-Dioctyl-9*H*-fluorene-2,7-diyl)dibenzaldehyde (3b). 2,7-Dibromo-9,9-dioctyl-9*H*-fluorene (**1b**) (1.15 g, 2.09 mmol), benzaldehyde **2** (1.13 g, 4.87 mmol), Cs_2CO_3 (9.70 g, 30.0 mmol), and $Pd(PPh_3)_4$ (0.28 g, 0.24 mmol) were reacted under the same conditions as described in the synthesis of **3a** to yield compound **3b** (1.10 g, 1.83 mmol, 87%) as a pale yellow solid: ^{1}H NMR (300 MHz, $CDCl^5$) δ 10.09 (s, 2H), 7.99 (d, J = 8.1 Hz, 4H), 7.86–7.83 (m, 6H), 7.68–7.61 (m, 4H), 2.10–2.04 (m, 4H), 1.19–1.03 (m, 24H), 0.78 (t, J = 6.8 Hz, 6H). The ^{1}H NMR data is consistent with the literature reported values.[28]

4,4′-(9,9-Dihexyl-9H-fluorene-2,7-diyl)dibenzaldehyde (3c). 2,7-Dibromo-9,9-dihexyl-9H-fluorene (**1c**) (1.00 g, 2.03 mmol), benzaldehyde **2** (1.07 g, 4.60 mmol), Cs_2CO_3 (4.40 g, 13.5 mmol), and $Pd(PPh_3)_4$ (0.22 g, 0.19 mmol) were reacted under the same conditions as described in the synthesis of **3a** to yield compound **3c** (0.90 g, 1.66 mmol, 86%) a pale yellow solid: ^{1}H NMR (300 MHz, $CDCl_3$) δ 10.08 (s, 2H), 7.99 (d, J = 8.4 Hz, 4H), 7.85–7.82 (m, 6H), 7.67–7.64 (m, 4H), 2.11–2.06 (m, 4H), 1.19–0.98 (m, 16H), 0.75 (t, J = 6.8 Hz, 6H). The ^{1}H NMR data is consistent with the literature reported values.[28]

Bis(DTF)-fluorene 5a. Dibenzaldehyde **3a** (1.00 g, 1.52 mmol), thione **4** (1.75 g, 3.66 mmol), and $P(OMe)_3$ (30 mL) were added to a 100 mL round-bottom flask. The mixture was heated to 145 °C and kept at this temperature for 5 h. Then $P(OMe)_3$ was removed by vacuum distillation, and the crude product was purified through silica column chromatography (hexanes) to give **5a** (1.27 g, 0.83 mmol, 55%) as a yellow oil: IR (neat) 2952, 2919, 2849, 1569, 1544, 1463, 818 cm^{-1}; ^{1}H NMR (300 MHz, $CDCl_3$) δ 7.75 (d, J = 7.9 Hz, 2H), 7.68 (d, J = 8.4 Hz, 4H), 7.61–7.57 (m, 4H), 7.32 (d, J = 8.4 Hz, 4H), 6.52 (s, 2H), 2.86–2.81 (m, 8H), 1.73–1.59 (m, 8H), 1.48–1.00 (m, 96H), 0.90–0.78 (m, 18H); ^{13}C NMR (75 MHz, CD_2Cl_2) δ 151.9, 140.2, 139.5, 138.9, 135.4, 132.5, 127.7, 127.33, 127,27, 125.9, 125.0, 121.3, 120.2, 114.1, 50.4, 40.6, 36.3, 36.2, 32.05, 32.04, 32.00, 31.7, 31.1, 30.2, 30.0, 29.9, 29.71, 29.68, 29.65, 29.47, 29.46, 29.40, 29.37, 29.3, 29.2, 28.73, 28.71, 22.82, 22.80, 22.78, 14.3, 14.2; HRMS [M + H]$^+$ calcd for $C_{93}H_{143}S_8$ 1515.8955, found 1515.8929.

Bis(DTF)-fluorene 5b. Dibenzaldehyde **3b** (0.40 g, 0.66 mmol), thione **4** (0.76 g, 1.60 mmol), and $P(OMe)_3$ (20 mL) were reacted under the same conditions as described in the synthesis of **5a** to give compound **5b** (0.70 g, 0.48 mmol, 72%) as a yellow oil: IR (neat) 2952, 2920, 2850, 1681, 1569, 1463, 1087, 819 cm^{-1}; ^{1}H NMR (300 MHz, $CDCl_3$) δ 7.76 (d, J = 7.9 Hz, 2H), 7.68 (d, J = 8.4 Hz, 4H), 7.61–7.57 (m, 4H), 7.32 (d, J = 8.4 Hz, 4H), 6.52 (s, 2H), 2.86–2.81 (m, 8H), 2.06–2.97 (m, 4H) 1.73–1.56 (m, 8H), 1.49–0.97 (m, 80H), 0.92–0.75 (m, 18H); ^{13}C NMR (75 MHz, $CDCl_3$) δ 151.9, 140.2, 139.6, 138.9, 135.4, 132.56, 127.65, 127.33, 127.29, 125.90, 125.00, 121.31, 120.18, 114.11, 55.4, 40.6, 36.3, 36.2, 32.0, 31.9, 30.2, 30.0, 29.9, 29.71, 29.69, 29.48, 29.47, 29.4, 29.3, 28.7, 24.0, 22.8, 22.7, 14.3, 14.2; HRMS [M + H]$^+$ calcd for $C_{89}H_{135}S_8$ 1459.8329, found 1459.8292.

Bis(DTF)-fluorene 5c. Dibenzaldehyde **3c** (0.57 g, 0.99 mmol), thione **4** (1.30 g, 2.25 mmol), and $P(OMe)_3$ (20 mL) were reacted under the same conditions as described in the synthesis of **5a** to give compound **5c** (0.95 g, 0.62 mmol, 62%) as a yellow oil: IR (neat) 3023, 2952, 2920, 2850, 1569, 1544, 1463, 818 cm^{-1}; ^{1}H NMR (300 MHz, $CDCl_3$) δ 7.75 (d, J = 8.0 Hz, 2H), 7.68 (d, J = 8.4 Hz, 4H), 7.63–7.54 (m, 4H), 7.32 (d, J = 8.4 Hz, 4H), 6.52 (s, 2H), 2.86–2.81 (m, 8H), 2.09–1.96 (m, 4H), 1.72–1.59 (m, 8H), 1.50–0.99 (m, 72H), 0.92–0.70 (m, 18H); ^{13}C NMR (75 MHz, $CDCl_3$) δ 151.9, 140.2, 139.5, 138.9, 135.4, 132.6, 127.7, 127.33, 127.27, 125.5, 125.0, 121.3, 120.2, 114.1, 55.4, 40.6, 36.3, 36.2, 32.0, 31.6, 30.0, 29.9, 29.71, 29.68, 29.47, 29.46, 29.3, 28.73, 28.70, 23.9, 22.8, 22.7, 14.3, 14.1; HRMS [M + H]$^+$ calcd for $C_{85}H_{127}S_8$ 1403.7703, found 1403.7718.

TTFV–Fluorene Co-oligomer 6a. To a solution of compound **5a** (0.11 g, 0.072 mmol) in CH_2Cl_2 (10 mL) were added iodine chips (0.050 g, 0.20 mmol). The resulting dark solution was stirred at room temperature for 5 h. After that, a saturated aqueous solution of $Na_2S_2O_3$ (10 mL) was added to the dark solution, and the mixture was stirred for another 3 h at room temperature. The resulting yellow organic layer was separated, washed with water, dried over $MgSO_4$, and concentrated under reduced pressure. The resulting crude product was subjected to silica gel column chromatography (hexanes/CH_2Cl_2, 4:1), giving co-oligomer **6a** (0.066 g, 59%) as a yellow oil: IR (neat) 2953, 2920, 2850, 1463, 1054, 816 cm^{-1}; ^{1}H NMR (300 MHz, $CDCl_3$) δ 7.77–7.47 (m, 36H), 7.34–7.26 (m, 4H), 6.50 (s, 2H), 2.89–2.70 (m, 26H), 2.08–1.87 (m, 10H), 1.74–1.55 (m, 26H), 1.49–0.95 (m, 272H), 0.92–0.75 (m, 64H); ^{13}C NMR (75 MHz, $CDCl_3$) δ 151.9, 151.8, 140.2, 139.8, 139.5, 138.9, 136.8, 136.0, 135.5, 135.4, 132.5, 129.0, 127.7, 127.32, 127.27, 127.1, 126.9, 125.9, 125.3, 125.0, 124.3, 121.3, 120.1, 114.1, 55.4, 40.7, 36.3, 36.2, 36.1, 32.08, 32.06, 32.0, 30.2, 30.0, 29.87, 29.85, 29.74, 29.72, 29.69, 29.64, 29.53, 29.48, 29.39, 29.35, 29.31, 28.75, 28.71, 24.0, 22.84, 22.79, 14.28, 14.26; GPC M_n = 8200, M_w = 11119, PDI = 1.35.

TTFV–Fluorene Co-oligomer 6b. Compound **5b** (0.10 g, 0.068 mmol) and iodine (0.050 g, 0.20 mmol) were reacted in CH_2Cl_2 (10 mL) under the same conditions as described in the synthesis of **6a** to

DOI: 10.1021/acs.joc.5b00792
J. Org. Chem. XXXX, XXX, XXX–XXX

give co-oligomer **6b** (0.067 g, 67%) as a yellow oil: IR (neat) 2952, 2920, 2850, 1463, 1434, 815 cm^{-1}; ^1H NMR (300 MHz, $CDCl_3$) δ 7.74−7.45 (m, 70H), 7.32−7.28 (m, 4H), 6.50 (s, 2H), 2.88−2.73 (m, 42H), 2.06−1.92 (m, 20H), 1.70−1.54 (m, 48H), 1.44−0.96 (m, 460H), 0.89−0.72 (m, 120H); ^{13}C NMR (75 MHz, $CDCl_3$) δ 151.84, 151.80, 140.2, 139.8, 139.5, 138.9, 136.8, 136.1, 136.0, 135.4, 132.6, 129.0, 127.33, 127.28, 127.1, 125.9, 125.3, 125.0, 124.3, 121.3, 120.2, 114.1, 55.4, 40.7, 36.3, 36.2, 36.1, 34.8, 32.1, 31.9, 31.8, 31.1, 30.2, 30.0, 29.9, 29.8, 29.72, 29.69, 29.53, 29.49, 29.4, 29.3, 29.2, 28.8, 28.7, 25.4, 24.0, 22.85, 22.82, 22.7, 20.9, 14.3, 14.2; GPC M_n = 7961, M_w = 12303, PDI = 1.54.

TTFV−Fluorene Co-oligomer 6c. Compound **5c** (0.060 g, 0.043 mmol) and iodine (0.030 g, 0.12 mmol) were reacted in CH_2Cl_2 (10 mL) under the same conditions as described in the synthesis of **6a** to give co-oligomer **6c** (0.040 g, 66%) as a yellow oil: IR (neat) 2952, 2920, 2850, 1463, 1433, 815 cm^{-1}; ^1H NMR (300 MHz, $CDCl_3$) δ 7.76−7.48 (m, 74H), 7.34−7.27 (m, 4H), 6.51 (s, 2H), 2.91−2.73 (m, 44H), 2.07−1.90 (m, 20H), 1.73−1.54 (m, 50H), 1.49−0.95 (m, 420H), 0.93−0.67 (m, 126H); ^{13}C NMR (75 MHz, $CDCl_3$) δ 151.9, 151.8, 140.2, 139.8, 139.5, 138.9, 136.8, 136.0, 135.4, 132.6, 128.9, 127.6, 127.33, 127.27, 127.1, 125.9, 125.3, 125.0, 124.33, 121.27, 120.1, 114.1, 55.37, 55.35, 53.6, 40.7, 36.3, 36.2, 36.1, 32.1, 31.6, 30.0, 29.9, 29.8, 29.74, 29.71, 29.68, 29.52, 29.48, 29.46, 29.37, 29.35, 29.30, 28.8, 28.74, 28.70, 24.0, 22.8, 22.7, 14.3, 14.1; GPC: M_n = 4932, M_w = 6865, PDI = 1.39.

DTF−Fluorene 7. Compound **3b** (0.32 g, 0.53 mmol), thione **4** (0.23 g, 0.48 mmol), and $P(OMe)_3$ (15 mL) were reacted at 125 °C for 3 h under the same conditions as described in the synthesis of **5a**. The obtained crude product was purified by silica column chromatography (hexanes/CH_2Cl_2, 4:1) to afford compound **7** (0.27 g, 0.26 mmol, 50%) as a yellow oil: FTIR (neat) 2952, 2921, 2851, 1701, 1601, 1568, 1545, 1464, 1254, 1210, 844, 815 cm^{-1}; ^1H NMR (300 MHz, $CDCl_3$) δ 10.0(s, 1H), 7.98 (d, J = 8.3 Hz, 2H), 7.89−7.75 (m, 4H), 7.73−7.54 (m, 6H), 7.33 (d, J = 8.4 Hz, 2H), 6.53 (s, 1H), 2.84 (t, J = 7.3 Hz, 4H), 2.10−1.98 (m, 4H), 1.74−1.60 (m, 4H), 1.48−0.99 (m, 52H), 0.94−0.73 (m, 12H); ^{13}C NMR (75 MHz, $CDCl_3$) δ 192.1, 152.1, 152.0, 147.8, 141.5, 140.05, 139.77, 138.76, 138.52, 135.54, 135.17, 132.7, 130.4, 127.8, 127.7, 127.34, 127.32, 126.6, 126.0, 125.0, 121.8, 121.4, 120.5, 120.4, 114.0, 55.5, 40.5, 36.3, 36.2, 32.1, 31.9, 30.1, 30.0, 29.9, 29.72, 29.69, 29.5, 29.33, 29.31, 28.74, 28.72, 23.9, 22.8, 22.7, 14.3, 14.2; HRMS $[M + H]^+$ calcd for $C_{66}H_{93}OS_4$ 1029.6109, found 1029.6112.

TTFV−Fluorene 8. Compound **7** (0.90 g, 0.87 mmol) and iodine (0.66 g, 2.6 mmol) were added in CH_2Cl_2 (15 mL), and the mixture was stirred at room temperature for 5 h. A saturated aqueous solution of $Na_2S_2O_3$ was added, and the resulting mixture was stirred at room temperature for another 1 h. The organic layer was separated, washed with H_2O, dried over $MgSO_4$, and concentrated under vacuum. The crude product obtained was purified through silica column chromatography (hexanes/CH_2Cl_2, 2:3) to yield compound **8** (0.58 g, 0.28 mmol, 65%) as a yellow oil: FTIR (neat) 2953, 2924, 2853, 1702, 1602, 1465, 1210, 1168, 815 cm^{-1}; ^1H NMR (300 MHz, $CDCl_3$) δ 10.0 (s, 2H), 7.98 (d, J = 8.4 Hz, 4H), 7.88−7.74 (m, 8H), 7.68−7.65 (m, 6H), 7.60−7.56 (m, 10H), 2.90−2.76 (m, 8H), 2.09−1.97 (m, 8H), 9.83−1.58 (m, 8H), 1.49−0.98 (m, 104H), 0.92−0.72 (m, 24H); ^{13}C NMR (75 MHz, $CDCl_3$) δ 192.1, 152.1, 151.9, 147.8, 141.5, 140.0, 139.8, 139.6, 138.5, 137.0, 136.2, 135.2, 130.4, 129.0, 128.9, 127.8, 127.4, 127.1, 126.6, 126.0, 125.3, 124.2, 121.8, 121.4, 120.45, 120.36, 55.5, 40.6, 36.3, 36.2, 32.1, 31.9, 30.1, 29.9, 29.8, 29.53, 29.49, 29.3, 28.8, 28.7, 24.0, 22.8, 22.7, 14.3, 14.2.; HRMS $[M + H]^+$ calcd for $C1_{32}H_{183}O_2S_8$ 2056.1984, found 2056.1924.

TTFV−Fluorene 9. Compound **8** (0.35 g, 0.17 mmol), thione **4** (0.24 g, 0.51 mmol), and $P(OMe)_3$ (15 mL) were reacted under the same conditions as described in the synthesis of **7** to afford compound **9** (0.28 g, 0.096 mmol, 56%) as a yellow oil: FTIR (neat) 2953, 2923, 1464, 817 cm^{-1}; ^1H NMR (300 MHz, $CDCl_3$) δ 7.74 (d, J = 7.8 Hz, 4H), 7.69−7.56 (m, 20H), 7.32 (d, J = 8.5 Hz, 4H), 6.52 (s, 2H), 2.88−2.78 (m, 16H), 2.06−1.95 (m, 8H), 1.75−1.57 (m, 16H), 1.49−0.99 (m, 160H), 0.94−0.76 (m, 36H); ^{13}C NMR (75 MHz, $CDCl_3$) δ 151.9, 151.8, 140.2, 139.8, 139.5, 138.9, 136.8, 136.0, 135.4, 132.5, 129.0, 127.6, 127.32, 127.28, 127.1, 125.9, 125.3, 125.0, 124.3, 121.31, 121.28, 120.2, 114.1, 55.4, 40.7, 36.3, 36.2, 36.1, 34.8, 34.7, 32.1, 31.9, 31.7, 30.2, 30.0, 29.8, 29.74, 29.71, 29.68, 29.52, 29.48, 29.46, 29.36, 29.34, 29.30, 29.2, 28.8, 28.73, 28.70, 27.1, 25.4, 23.9, 22.84, 22.81, 22.7, 14.3, 14.2; HRMS $[M + H]^+$ calcd for $C_{178}H_{267}S_{16}$ 2916.6424, found 2916.6499.

TTFV−Fluorene Macrocycle 10. Compound **9** (0.080 g, 0.027 mmol) and iodine (0.020 g, 0.081 mmol) were reacted in CH_2Cl_2 (5 mL) under the same conditions as described in the synthesis of **6a** to yield compound **10** (0.030 g, 37%) as a yellow oil: FTIR (neat) 2953, 2923, 2852, 1464, 1260, 1092, 1017, 814, 803 cm^{-1}; ^1H NMR (300 MHz, $CDCl_3$) δ 7.71−7.46 (m, 7H), 2.96−2.64 (m, 8H), 1.92−0.92 (m, 40H), 0.86−0.74 (m, 9H); GPC M_n = 3126, M_w = 7297, PDI = 2.33.

■ ASSOCIATED CONTENT

Supporting Information

NMR spectra of all new compounds. The Supporting Information is available free of charge on the ACS Publications website at DOI: 10.1021/acs.joc.5b00792.

■ AUTHOR INFORMATION

Corresponding Author

*Tel: +1 709 864 8747. Fax:+1 709 864 3702. E-mail: yuming@mun.ca.

Notes

The authors declare no competing financial interest.

■ ACKNOWLEDGMENTS

We acknowledge the Natural Sciences and Engineering Research Council of Canada (NSERC), Canada Foundation for Innovation (CFI), and Memorial University for financial support. Prof. A. Adronov and Mr. S. Liang of McMaster University are acknowledged for their assistance in GPC analysis.

■ REFERENCES

(1) (a) Skotheim, T. A., Elsenbaumer, R. L., Reynolds, J. R., Eds. *Handbook of Conducting Polymers*, 2nd ed.; Marcel Dekker: New York, 1997. (b) Hirao, T., Ed. *Redox Systems Under Nano-Space Control: Nano-Space Control and Its Applications*; Springer: Berlin, 2006. (c) Mishra, A.; Ma, C.-Q.; Bäuerle, P. *Chem. Rev.* **2009**, *109*, 1141−1276. (d) Inzelt, G. *Conducting Polymers: A New Era in Electrochemistry*, 2nd ed.; Springer: Berlin, 2012. (e) Hirao, T., Ed. *Functionalized Redox Systems: Synthetic Reactions and Design of π- and Bio-Conjugates*; Springer: Heidelberg, 2015.

(2) (a) Luo, L.; Benameur, A.; Brignou, P.; Choi, S. H.; Rigaut, S.; Frisbie, C. D. *J. Phys. Chem. C* **2011**, *115*, 19955−19961; (b) Hortholary, C.; Coudret, C. *J. Org. Chem.* **2003**, *68*, 2167−2174;(c) Chen, C.-P.; Luo, W.-R.; Chen, C.-N.; Wu, S.-M.; Hsieh, S.; Chiang, C.-M.; Dong, T.-Y. *Langmuir* **2013**, *29*, 3106−3115; (d) Schubert, C.; Margraf, J. T.; Clark, T.; Guldi, D. M. *Chem. Soc. Rev.* **2015**, *44*, 988−998.

(3) (a) Shaibu, B. S.; Lin, S.-H.; Lin, C.-Y.; Wong, K.-T.; Liu, R.-S. *J. Org. Chem.* **2011**, *76*, 1054−1061;(b) Segura, J. L.; Martín, N.; Guldi, D. M. *Chem. Soc. Rev.* **2005**, *34*, 31−47;(c) Alévêque, O.; Leriche, P.; Cocherel, N.; Frère, P.; Cravino, A.; Roncali, J. *Sol. Energy Mater. Sol. Cells* **2008**, *92*, 1170−1174;(d) Guo, K.; Yan, K.; Lu, X.; Qiu, Y.; Liu, Z.; Sun, J.; Yan, F.; Guo, W.; Yang, S. *Org. Lett.* **2012**, *14*, 2214−2217; (e) Wan, Z.; Jia, C.; Duan, Y.; Chen, X.; Lin, Y.; Shi, Y. *Org. Electron.* **2013**, *14*, 2132−2138.

(4) (a) Sönmez, G.; Schwendeman, I.; Schottland, P.; Zong, K.; Reynolds, J. R. *Macromolecules* **2003**, *36*, 639−647;(b) Nishida, J.-i.; Miyagawa, T.; Yamashita, Y. *Org. Lett.* **2004**, *6*, 2523−2526;(c) Wang, X.; Ng, J. K.-P.; Jia, P.; Lin, T.; Cho, C. M.; Xu, J.; Lu, X.; He, C.

DOI: 10.1021/acs.joc.5b00792
J. Org. Chem. XXXX, XXX, XXX−XXX

Macromolecules **2009**, *42*, 5534−5544;(d) Beaujuge, P. M.; Reynolds, J. R. *Chem. Rev.* **2010**, *110*, 268−320.
(5) (a) Chen, G.; Mahmud, I.; Dawe, L. N.; Zhao, Y. *Org. Lett.* **2010**, *12*, 704−707;(b) Chen, G.; Mahmud, I.; Dawe, L. N.; Daniels, L. M.; Zhao, Y. *J. Org. Chem.* **2011**, *76*, 2701−2715.
(6) (a) Xu, B. Q.; Li, X. L.; Xiao, X. Y.; Sakaguchi, H.; Tao, N. *Nano Lett.* **2005**, *5*, 1491−1495;(b) Tam, I. W.; Yan, J.; Breslow, R. *Org. Lett.* **2006**, *8*, 183−185;(c) Ohtake, T.; Tanaka, H.; Matsumoto, T.; Kimura, M.; Ohta, A. *J. Org. Chem.* **2014**, *79*, 6590−6602.
(7) (a) McQuade, D. T.; Pullen, A. E.; Swager, T. M. *Chem. Rev.* **2000**, *100*, 2537−2574;(b) Huang, J.; Virji, S.; Weiller, B. H.; Kaner, R. B. *J. Am. Chem. Soc.* **2003**, *125*, 314−315;(c) Liu, H.; Kameoka, J.; Czaplewski, D. A.; Craighead, H. G. *Nano Lett.* **2004**, *4*, 671−675; (d) Liu, B.; Bazan, G. C. *J. Am. Chem. Soc.* **2006**, *128*, 1188−1196.
(8) (a) Wang, F.; Lai, Y.-H.; Han, M.-Y. *Macromolecules* **2004**, *37*, 3222−3230;(b) Amir, E.; Amir, R. J.; Campos, L. M.; Hawker, C. J. *J. Am. Chem. Soc.* **2011**, *133*, 10046−10049;(c) Ohtake, T.; Tanaka, H.; Matsumoto, T.; Ohta, A.; Kimura, M. *Langmuir* **2014**, *30*, 14680−14685.
(9) (a) Liang, S.; Chen, G.; Peddle, J.; Zhao, Y. *Chem. Commun.* **2012**, *48*, 3100−3102;(b) Liang, S.; Chen, G.; Zhao, Y. *J. Mater. Chem. C* **2013**, *1*, 5477−5490;(c) Liang, S.; Zhao, Y.; Adronov, A. *J. Am. Chem. Soc.* **2014**, *136*, 970−977.
(10) (a) Yamada, J.-i., Sugimoto, T., Eds. *TTF Chemistry: Fundamentals and Applications of Tetrathiafulvalene*; Springer: Berlin, 2004. (b) Segura, J. L.; Martín, N. *Angew. Chem., Int. Ed.* **2001**, *40*, 1372−1409;(c) Canevet, D.; Sallé, M.; Zhang, G.; Zhang, D.; Zhu, D. *Chem. Commun.* **2009**, 2245−2269.
(11) (a) Moore, A. J.; Bryce, M. R.; Ando, D. J.; Hursthouse, M. B. *J. Chem. Soc., Chem. Commun.* **1991**, 320−321;(b) Moore, A. J.; Bryce, M. R. *Tetrahedron Lett.* **1992**, *33*, 1373−1376;(c) Yu, L.; Zhu, D. *Chem. Commun.* **1997**, 787−788;(d) Bellec, N.; Boubekeur, K.; Carlier, R.; Hapiot, P.; Lorcy, D.; Tallec, A. *J. Phys. Chem. A* **2000**, *104*, 9750−9759;(e) Carlier, R.; Hapiot, P.; Lorcy, D.; Robert, A.; Tallec, A. *Electrochim. Acta* **2001**, *46*, 3269−3277;(f) Roncali, J. *J. Mater. Chem.* **1997**, *7*, 2307−2321;(g) Bendikov, M.; Wudl, F.; Perepichka, D. F. *Chem. Rev.* **2004**, *104*, 4891−4946;(h) Zhao, Y.; Chen, G.; Mulla, K.; Mahmud, I.; Liang, S.; Dongare, P.; Thompson, D. W.; Dawe, L. N.; Bouzan, S. *Pure Appl. Chem.* **2012**, *84*, 1005−1025.
(12) (a) Inagi, S.; Naka, K.; Chujo, Y. *J. Mater. Chem.* **2007**, *17*, 4122−4135;(b) Inagi, S.; Naka, K.; Iida, D.; Chujo, Y. *Polym. J.* **2006**, *38*, 1146−1151;(c) Naka, K.; Inagi, S.; Chujo, Y. *J. Polym. Sci., Part A: Polym. Chem.* **2005**, *43*, 4600−4608;(d) Lorcy, D.; Mattiello, L.; Poriel, C.; Rault-Berthelot, J. *J. Electroanal. Chem.* **2002**, *530*, 33−39.
(13) (a) Guerro, M.; Carlier, R.; Boubekeur, K.; Lorcy, D.; Hapiot, P. *J. Am. Chem. Soc.* **2003**, *125*, 3159−3167;(b) Guerro, M.; Roisnel, T.; Pellon, P.; Lorcy, D. *Inorg. Chem.* **2005**, *44*, 3347−3355;(c) Gontier, E.; Bellec, N.; Brignou, P.; Gohier, A.; Guerro, M.; Roisnel, T.; Lorcy, D. *Org. Lett.* **2010**, *12*, 2386−2389;(d) Lorcy, D.; Guerro, M.; Bergamini, J.-F.; Hapiot, P. *J. Phys. Chem. B* **2013**, *117*, 5188−5194.
(14) Chen, G.; Zhao, Y. *Org. Lett.* **2014**, *16*, 668−671.
(15) (a) Massue, J.; Bellec, N.; Guerro, M.; Bergamini, J.-F.; Hapiot, P.; Lorcy, D. *J. Org. Chem.* **2007**, *72*, 4655−4662;(b) Mulla, K.; Dongare, P.; Thompson, D. W.; Zhao, Y. *Org. Biomol. Chem.* **2012**, *10*, 2542−2544;(c) Mulla, K.; Shaik, H.; Thompson, D. W.; Zhao, Y. *Org. Lett.* **2013**, *15*, 4532−4535;(d) Mulla, K.; Zhao, Y. *Tetrahedron Lett.* **2014**, *55*, 382−386.
(16) Hapiot, P.; Lorcy, D.; Tallec, A.; Carlier, R.; Robert, A. *J. Phys. Chem.* **1996**, *100*, 14823−14827.
(17) Benahmed-Gasmi, A.; Frère, P.; Roncali, J.; Elandaloussi, E.; Orduna, J.; Garin, J.; Jubault, M.; Gorgues, A. *Tetrahedron Lett.* **1995**, *36*, 2983−2986.
(18) (a) Yamashita, Y.; Tomura, M.; Zaman, M. B.; Imaeda, K. *Chem. Commun.* **1998**, 1657−1658;(b) Bouzan, S.; Chen, G.; Mulla, K.; Dawe, L. N.; Zhao, Y. *Org. Biomol. Chem.* **2012**, *10*, 7673−7676; (c) Bouzan, S.; Dawe, L. N.; Zhao, Y. *Tetrahedron Lett.* **2013**, *54*, 4666−4669;(d) Woolridge, K.; Goncalves, L. C.; Bouzan, S.; Chen, G.; Zhao, Y. *Tetrahedron Lett.* **2014**, *55*, 6362−6366.
(19) (a) Massue, J.; Ghilane, J.; Bellec, N.; Lorcy, D.; Hapiot, P. *Electrochem. Commun.* **2007**, *9*, 677−682;(b) Younes, E. A.; Williams, K.-L. M.; Walsh, J. C.; Schneider, C. M.; Bodwell, G. J.; Zhao, Y. *RSC Adv.* **2015**, *5*, 23952−23956;(c) Inagi, S.; Naka, K.; Chujo, Y. *J. Mater. Chem.* **2007**, *17*, 4122−4135.
(20) González, S.; Martín, N.; Sánchez, L.; Segura, J. L.; Seoane, C.; Fonseca, I.; Cano, F. H.; Sedó, J.; Vidal-Gancedo, J.; Rovira, C. *J. Org. Chem.* **1999**, *64*, 3498−3506.
(21) Miyaura, N.; Suzuki, A. *Chem. Rev.* **1995**, *95*, 2457−2483.
(22) Christensen, C. A.; Batsanov, A. S.; Bryce, M. R. *J. Org. Chem.* **2007**, *72*, 1301−1308.
(23) Gosser, D. K. *Cyclic Voltammetry: Simulation and Analysis of Reaction Mechanisms*; Wiley-VCH: New York, 1993.
(24) Saito, R.; Dresselhaus, G.; Dresselhaus, M. S. *Physical Properties of Carbon Nanotubes*; Imperial College Press: London, 1998. Meyyappan, M. *Carbon Nanotubes: Science and Applications*; CRC Press: Boca Raton, 2005. Guldi, D. M.; Martín, N. *Carbon Nanotubes and Related Structures: Synthesis, Characterization, Functionalization, and Applications*; Wiley-VCH: Weinheim, 2010.
(25) (a) Kürti, J.; Kresse, G.; Kuzmany, H. *Phys. Rev. B: Condens. Matter Mater. Phys.* **1998**, *58*, R8869−R8872;(b) Maultzsch, J.; Telg, H.; Reich, S.; Thomsen, C. *Phys. Rev. B: Condens. Matter Mater. Phys.* **2005**, *72*, 205438.
(26) Jorio, A.; Saito, R.; Hafner, J. H.; Lieber, C. M.; Hunter, M.; McClure, T.; Dresselhaus, G.; Dresselhaus, M. S. *Phys. Rev. Lett.* **2001**, *86*, 1118−1121.
(27) (a) Mulla, K.; Zhao, Y. *J. Mater. Chem. C* **2013**, *1*, 5116−5127; (b) Wang, D.; Chen, L. *Nano Lett.* **2007**, *7*, 1480−1484;(c) Zhang, Z.; Che, Y.; Smaldone, R. A.; Xu, M.; Bunes, B. R.; Moore, J. S.; Zang, L. *J. Am. Chem. Soc.* **2010**, *132*, 14113−14117;(d) Pochorovski, I.; Wang, H.; Feldblyum, J. I.; Zhang, X.; Antaris, A. L.; Bao, Z. *J. Am. Chem. Soc.* **2015**, *137*, 4328−4331.
(28) Long, Y.; Chen, H.; Yang, Y.; Wang, H.; Yang, Y.; Li, N.; Li, K.; Pei, J.; Liu, F. *Macromolecules* **2009**, *42*, 6501−6509.

DOI: 10.1021/acs.joc.5b00792
J. Org. Chem. XXXX, XXX, XXX−XXX